RESEARCH ARTICLE

Preparation and characterization of selenide starch

Jin Li*, Jie Gao, Peiling Duan

College of Pharmacy, Zhengzhou Railway Vocational & Technical College, Zhengzhou, Henan, China

Received: April 20, 2023; **accepted:** May 20, 2023.

Traditional cereal starch has high digestibility. Therefore, after ingestion, it is easy to cause a rapid increase in blood sugar in a short period of time, which may cause harm to the human body. Mung bean starch has strong detoxification effects due to its rich antioxidant compounds. This study was to prepare mung bean resistant starch (MB-RS4) by esterification of mung bean starch (MBS) with citric acid, and further selenized mung bean resistant starch (MB-RS4·Se (IV)) by using nitrate sodium selenite. The structural characterization and biological activity of MB-RS4·Se (IV) were then analyzed. The results demonstrated that the optimal preparation process conditions for MB-RS4·Se (IV) were 66℃ for 3.5 hours with the volume fraction of 0.5% nitric acid. The maximum absorption peak of MB-RS4·Se (IV) after selenization was at the wavelength of 220 nm with the maximum absorbance of 0.677. Its scavenging ability for O^{2-} and 2,2 '- diazodi (3-ethylbenzothiazoline-6-sulfonic acid) ion (ABTS+) reached the highest level at the mass concentration of 2 mg/mL, while its scavenging ability for OH was the highest at the mass concentration of 6 mg/mL. The IC_{50} of MB-RS4·Se (IV) was 2.68 mg/mL. The selenization modification transformed the non-inhibitory effect of MB-RS4 on α−glucose into the presence of inhibitory effect. Overall, MB-RS4·Se (IV) demonstrated high antioxidant and enzymatic properties. It showed high effectiveness in the actual elimination of free radicals in the human body *in vitro*.

Keywords: mung bean; resistant starch; biological activity; selenization.

***Corresponding author:** Jin Li, College of Pharmacy, Zhengzhou Railway Vocational & Technical College, Zhengzhou 451460, Henan, China. Email: lijin20083423@163.com.

Introduction

Resistant starch (RS) is a new type of dietary fiber that has emerged in recent years with significant effects on improving the structure of gut microbiota, promoting the proliferation of beneficial gut bacteria, and regulating hormone secretion levels and glucose and lipid metabolisms in the body. Therefore, it is often applied in the treatment of chronic diseases [1]. RS is a multifunctional dietary fiber. This dietary fiber cannot be directly digested and absorbed in the human body but is fermented by gut microbiota in the small intestine, which can regulate the structure of the gut microbiota [2]. The basic principle of the traditional preparation method of RS is to reduce the chain length of starch and change its molecular structure. Therefore, its crystal structure undergoes changes, preventing it from being digested [3]. However, although the conventionally prepared RS has certain biological activity, its actual effect is relatively single, and not significant. Therefore, modifying RS preparation has become a top priority to improve RS physicochemical properties. Many domestic and international studies have been conducted in-depth. Wang, *et al*. proposed a RS preparation method with strong *in vitro* anti digestion ability comparing to the other preparation methods and explored the optimal RS preparation conditions [4], which provided a new way to regulate the actual

digestibility of food. Arp, *et al*. developed a novel method for the preparation of RS by utilizing thermal and enzymatic modification methods [5], which also provided ideas for the preparation of low digestibility starch. Patterson, *et al*. conducted a detailed analysis of current preparation methods to propose RS suitable for human consumption [6], which laid the theoretical foundation for a new preparation method with moisture adjustment. Xu, *et al*. compared and analyzed the weight loss effects of RS extracted from two preparation methods [7]. While proposing the optimal method, it also provides assistance in reducing high fat in the human body. In addition, Denchai, *et al*. conducted a detailed analysis of rice starch at different temperatures to investigate the combined effects of parameters including starch retrogradation. The results provided the data for the storage time of resistant starch produced by retrogradation [8]. Ye, *et al*. explored a new method for resistant starch preparation by synthesizing resistant starch with citric acid esterification using the Danying extrusion method to reduce starch digestibility [9]. de Azevedo, *et al*. who focused on marine plastic waste prepared biological price reduced bioplastics with modified corn and potato starch [10], which provided assistance for sustainable environmental development. Li, *et al*. proposed a new type of resistant starch with dietary nutrition for the application of purple yam in hamster feeding to address the regulatory issue of hyperlipidemia in hamsters [11]. This study provided a theoretical basis for regulating the gut microbiota and laid the foundation for subsequent drug therapy. However, the current research on the preparation of RS has neither analyzed the coordination principle in esterified starch nor explored its actual inhibitory effect.

Selenium is an essential trace element for plant and animal growth, which cannot be synthesized by the body and is mainly obtained through food or supplements. Natural selenium can be divided into organic selenium and inorganic selenium according to its occurrence state. Compared to inorganic selenium, organic selenium has a stronger absorption capacity for the body [12]. Selenium polysaccharides have good biological activity and stability and have been widely used in selenium nutrition. Due to the low selenium content in natural selenium polysaccharides, selenization is necessary to obtain selenium rich organic selenium polysaccharides [13]. For the problems related to the diet nutrition of sows, on the basis of RS, Li, *et al*. used hydrogen selenide to synthesize selenoprotein that conformed to the diet of sows [14]. Zhang, *et al*. focused on the preparation of glutathione peroxidase and synthesized a new type of starch with selenium function through sodium hydrogen selenide reaction [15]. Pasaretti, *et al*. proposed a new type of thermoplastic starch composite material for plastic film preparation based on selenization treatment and mica clay to meet the actual needs of garden agriculture [16]. The effect of conventional preparation of RS is not significant. Therefore, modifying it with selenium can help improve its health benefits. The method of preparing MB-RS4·Se (IV) using nitric acid sodium selenite method is innovative in exploring the inhibition kinetics before and after improvement, which also provides a theoretical basis for industrial production and the research and development of functional foods.

For the purposes to slow down the digestion rate of traditional starch and balance the sugar metabolism in the human body, this study used citric acid to esterification mung bean starch (MBS) to prepare mung bean resistant starch (MB-RS4), and then, used nitrate sodium selenite to prepare selenized mung bean resistant starch (MB-RS4·Se (IV)). The results of this study would lay the foundation for the development of a functional starch formula that integrated the regulation of starch digestion performance and micronutrient enhancement and a theoretical foundation for subsequent industrial production and the development of functional foods.

Materials and Methods

Preparation of selenized mung bean starch

The mung bean resistant starch (MB-RS4) was first prepared by esterification of mung bean starch (MBS) with citric acid. Then selenized mung bean resistant starch (MB-RS4·Se (IV)) was prepared by adding nitric acid sodium selenite to MB-RS4 using the ester group in MB-RS4 as the coordination group. Briefly, 1.0 g of human selenidated dandelion polysaccharides (Sigma, St. Louis, Missouri, USA) was dissolved in 50 mL of nitric acid (HNO_3) before adding 1.0 g of sodium selenite (Na_2SeO_3) (Beijing Beihua Fine Chemicals Co., Ltd., Beijing, China) and 0.7 g of barium chloride (East China Reagent Factory, Shenyang, Liaoning, China). The reaction mixture was mixed at 66°C for 3.5 hours while 1 M sodium hydroxide (NaOH) solution (pH 7-8) was prepared and cooled down to room temperature. 0.5 mL of sodium sulfate (Na_2SO_4) was added to the reaction mixture and centrifuged at 4,000 rpm for 15 mins to remove barium ions. The supernatant was collected and dialyzed to remove the inorganic salt and excess Na_2SeO_3 in the reaction. The MB-RS4·Se (IV) was then obtained through the procedures of concentration, alcohol precipitation, and freeze-drying operations. The success rate of this method was calculated by using the following equation.

$$MB = \frac{G}{g} \times 100\% \quad (1)$$

where *MB* was the success rate. *G* was the actual mass of MB-RS4·Se (IV) (g). *g* was the actual mass of MB-RS4 (g). The selenium content in MB-RS4·Se (IV) was calculated below.

$$X = \frac{\delta}{v_3 \times G \times 1000} \quad (2)$$

where *X* was the selenium content. v_3 was the actual volume of the solution. δ was the value obtained by multiplying multiple indicators and was calculated by using equation (3) below.

$$\delta = \gamma \times v_2 \times v_1 \quad (3)$$

where γ was the actual mass concentration of selenium in the organic phase (mg/mL). v_2 was the actual total volume with indications. v_1 was the actual volume of the solution after constant volume. Then, the selenium standard curve and linear correlation coefficient based on spectrophotometry were expressed as follows.

$$\begin{cases} m = 19.38021 j - 0.04204 \\ R^2 = 0.9957 \end{cases} \quad (4)$$

where *m* was the selenium content. *j* was the absorbance. R^2 was the linear correlation coefficient.

Structure and physical properties of selenized mung bean starch

The structure and physical properties of MB-RS4·Se (IV) were determined by using ultraviolet spectroscopy (UV), Fourier transform infrared spectroscopy (FTIR), and X-ray diffraction analysis. Briefly, 2 mg/mL of sample was filtered through a small pore filter followed by scanning at the wavelength range of 190 - 400 nm using Specord 210 plus UV spectroscopy (DeChem-Tech. GmbH, Hamburg, Germany). Fourier transform infrared spectroscopy (FTIR) was performed by mixing 2 mg of the sample with 200 mg of potassium bromide (KBr) powder and then measured at 4,000 – 400/cm by using Nicolet 6700 FT-IR spectrometer (Thermo Fisher Scientific, Waltham, MA, USA). The dry and delicate samples were evenly dispersed and compacted within the plate frame, making the surface of the sample smooth and flat. After fixing the sample frame, the X-ray diffraction analysis was performed. The relative molecular weight and distribution were determined mainly by the effect of gel permeation chromatography (GPC) using Shimadzu LC20+RID20A (Shimadzu, Kyoto, Japan). The study applied narrow distribution polyethylene glycol (PEO) to produce a standardized curve relative correction method [17, 18]. The solubility measurement was calculated as follows.

$$D = \frac{r_1 - \omega}{r_1} \times 100\% \quad (5)$$

where *D* was the solubility. r_1 represented 2 g of sample. ω was the difference between the constant weight of the sample (r_4) and the weight of the centrifuge tube (r_2) and was calculated as follows.

$$\omega = r_4 - r_2 \quad (6)$$

The water holding capacity was determined based on the equation (7).

$$C = \frac{\xi}{r_4} \times 100\% \quad (7)$$

where *C* was the holding capacity. ξ was the difference between the weight of the sample after discarding the supernatant (r_3) and the weight of the centrifuge tube and was calculated as:

$$\xi = r_3 - r_2 \quad (8)$$

The measurement of transparency mainly involved accurately weighing 2.0 g of sample in a centrifuge tube and preparing it as a 2% reaction mixture by mixing starch and citric acid in a dry-to-dry ratio of 5:2). After mixing evenly, the reaction was heated in a 90°C water bath for 25 minutes to ensure that it could be fully gelatinized. After cooling down to room temperature, the reaction mixture was measured at 650 nm with the distilled water used as the control. The transparency *T*% was then calculated by using the following equation.

$$l = 2 - \log(T\%) \quad (9)$$

***In vitro* biological activity of selenized mung bean starch**

The hydroxyl radical was determined by using Fenton reaction to produce free radical burning shadow and track the absorbance degree of dianthoxyl free radical to monitor the actual reaction speed. The clearance rate was determined as follows.

$$Q = \frac{B}{B_0} \quad (10)$$

where Q was the clearance rate of hydroxyl radical. B_0 was the actual absorbance of the blank control at 510 nm. *B* was the difference in absorbance (B_1) between the blank control and the sample at 510 nm and was determined by equation (11).

$$B = B_0 - B_1 \quad (11)$$

The calculation of oxygen ion radical scavenging rate was similar to that of hydroxyl radical scavenging rate, except the different absorbance. Briefly, pyrogallol with the buffer and distill water were preheated at 25°C for 20 minutes before the absorbance values were measured at every 30 seconds at the wavelength of 325 nm. The stable 2,2'-azino-bis(3-ethylbenzothiazoline-6-sulfonic acid) ($ABTS^+$) radicals obtained by oxidation of 2,2'-diazo-bis(3-ethylbenzothiazoline-6-sulfonic acid) was determined by separating polysaccharides using boiling water method [18]. Its clearance rate was calculated below.

$$ABTS^+ = \left[1 - \frac{F}{F_0}\right] \times 100\% \quad (12)$$

where $ABTS^+$ was the $ABTS^+$ radical scavenging rate. F_0 was 1.2 mL of $ABTS^+$ diluent + 0.2 mL of anhydrous methanol. *F* was the difference between 0.2 mL of sample diluent + 1.2 mL of $ABTS^+$ diluent (F_1) and 0.2 mL of sample diluent + 1.2 mL of anhydrous methanol (F_2) as follows.

$$F = F_1 - F_2 \quad (13)$$

The determination of total antioxidant capacity was carried out by using a method to reduce iron ions. In the determination of *in vitro* anti

enzymatic properties, 1 g of the sample was mixed with 20 mL of 0.1 mol/L sodium acetate buffer and 5 mL of the mixture of porcine pancreatic α−glucosidase and α−amylase. The inhibition rate of glucosidase was calculated as follows by using acarbose as a positive control.

$$M = \left(1 - \frac{\alpha}{\beta}\right) \quad (14)$$

where α was the difference between the absorbance of the suppression group (samples and enzymes, H_1) and the absorbance of the control group (buffer solution, H_2). β was the difference between the absorbance of the sample base group (samples and ddH_2O, H_3) and the absorbance of the blank group (ddH_2O and buffer solution, H_0).

$$\begin{cases} \alpha = H_1 - H_2 \\ \beta = H_3 - H_0 \end{cases} \quad (15)$$

Statistical analysis

All experiments were set up in three parallel groups and the relevant data was represented by using mean ± standard deviation (SD). SPSS Statistics 25 (IBM, Armonk, New York, USA) and Microsoft Excel 2020 (Microsoft, Redmond, Washington, USA) were employed for statistical analysis. The actual significant difference was set as $P < 0.05$.

Results and discussion

The preparation process conditions and results of selenized mung bean starch

The effectiveness of MB-RS4·Se (IV) preparation process conditions, structure and physical properties, and *in vitro* biological activity were tested in this study. The corresponding single factor analysis was performed to determine the preparation process conditions and the results were shown in Figure 1. The reaction temperature demonstrated significant impact on the synthesis of MB-RS4·Se (IV) with the optimal temperature of 70℃, at which the selenium content tended to be saturated. The preparation success rate of MB-RS4·Se (IV) reached the highest of 23.35% at 4 hours of reaction with the selenium content of 2.04 mg/g. When the actual volume fraction of nitric acid was 0.5%, the success rate of MB-RS4·Se (IV) preparation and the selenium content reached the maximum values. MB-RS4 exhibited a completely transformation phenomenon when the mass ratio was 1:1. Overall, these single factors were important and affected the success rate of MB-RS4·Se (IV) preparation. To meet the production needs, after optimizing the process conditions, the mass fraction of HNO_3 was set at 0.5%, the material ratio was 1:1, and the reaction temperature and time were 66℃ and 3.5 hours. Following the above determined experimental conditions, the success rate of MB-RS4·Se (IV) preparation reached 26.451% and the content of selenium reached 2.21 mg/g. In addition, the modification process of MB-RS4·Se (IV) response surface was explored. Figure 2 demonstrated that the *P* values of both models were less than 0.01, indicating that the model had a very significant impact on the response value. The *P* values of the mismatched phase were both greater than 0.05, indicating that both models had a high degree of fit. These two models can be used to analyze and predict the actual success rate of selenization preparation and the actual content of selenium. The determination coefficients $R^2$of the two models were 0.987 and 0.999, which both were higher than 0.92. The corrected determination coefficients (R^2Adj) were 0.973 and 0.999 and both higher than 0.85, which indicated that the factors selected in both models had a significant impact on the variation of reaction values. Meanwhile, the signal-to-noise ratio of both models was greater than 4, indicating high reliability of these two models. Overall, both models showed high confidence levels and could well fit the relationship between the selected independent variables and response values.

The structure and physical properties of selenized mung bean starch

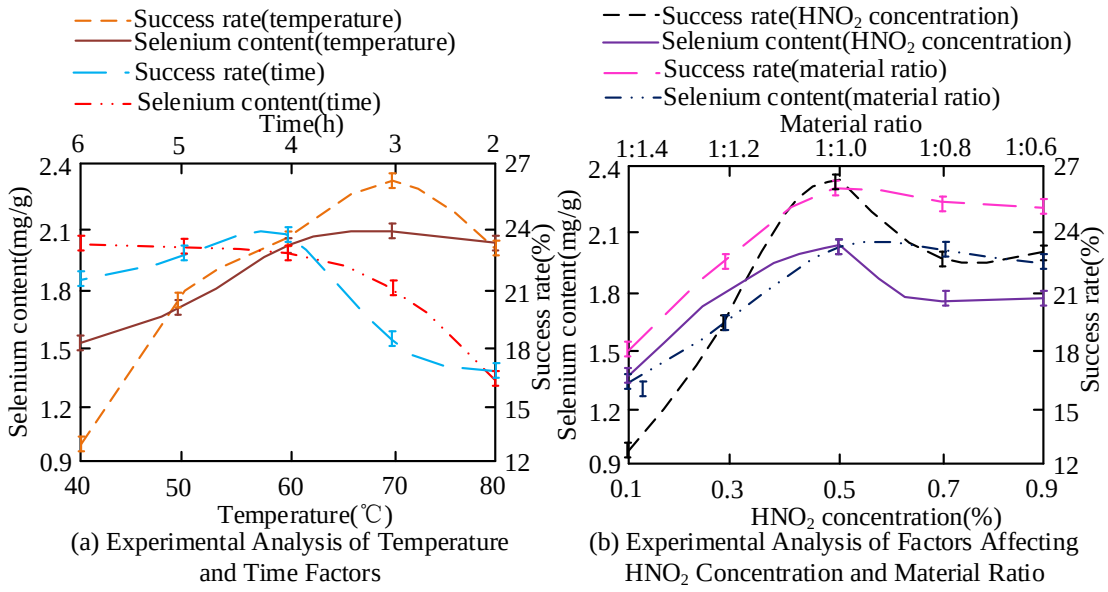

Figure 1. Single factor analysis of MB-RS4·Se (IV) preparation process conditions.

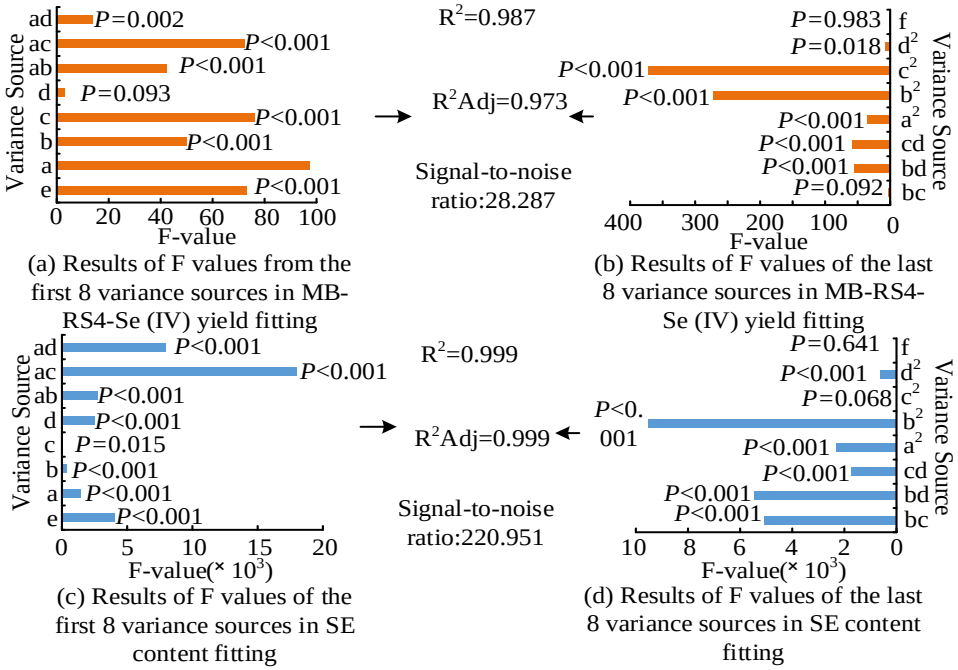

Figure 2. Modification process of MB-RS4·Se (IV) response surface. (Notes: a: HNO_3, b: material ratio, c: reaction temperature, d: reaction time, e: regression model, f: mismatch terms.)

The UV, FTIR, and X-ray diffraction patterns of MB-RS4 and MB-RS4·Se (IV) were analyzed (Figure 3). For UV study, Na_2SeO_3 exhibited a strong characteristic absorption peak at 225 nm, while MB-RS4·Se (IV) and MB-RS4 showed the maximum absorption peaks at 220 nm and 248 nm, and the maximum absorbances of 0.677 and 1.223, respectively. In FTIR analysis, the characteristic peak of MB-RS4·Se (IV) shifted red at 1745.23/cm, indicating that uronic acid esters

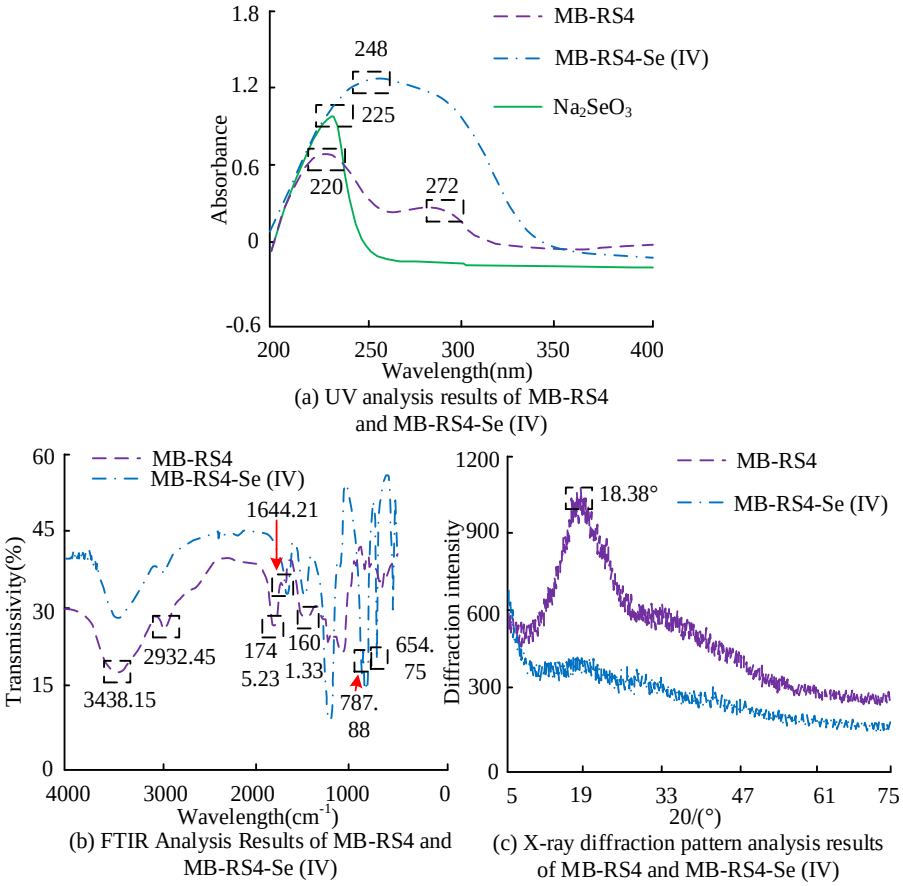

Figure 3. The results of UV, FTIR, and X-ray diffraction patterns of MB-RS4 and MB-RS4·Se (IV).

were involved in selenization. The reduction of the numbers of wave peaks between 1,000/cm and 800/cm after selenization indicated a structural change. In the analysis of X-ray diffraction patterns, MB-RS4·Se (IV) showed a loose state, indicating that its internal crystal structure had been destroyed. In addition, the gel permeation chromatography (GPC) and relative molecular weight analysis of MB-RS4 and MB-RS4·Se (IV) were performed to analyze relative molecular weight and distribution (Figure 4). The results showed that MB-RS4·Se (IV) exhibited only one component peak with a molecular weight of 8.012×10^3 g/mol. In the relative molecular weight analysis, there was a single component peak in MB-RS4·Se (IV) with the molecular weight ranged from 9.04×10^4 to 0.2×10^3 g/mol. The molecular weight showed good stability after selenization. In MB-RS4-Se (IV), selenization made the large molecular weight components changed into small molecular weight components due to the breaking of ester group and glycosidic bond, which would increase the proportion of small molecular weight segments. The results of relative molecular mass distribution before and after improvement were shown in Table 1. The number average and weight average of relative molecular weights of MB-RS4·Se (IV) were 2.26×10^2 g/mol and 1.20×10^2 g/mol, respectively, with a dispersion coefficient of 9.22. All three numbers were lower than that of MB-RS4 before modification. Overall, after selenization of MB-RS4, the dispersion rate significantly decreased, which indicated an improvement of its uniformity. The physical characteristics analysis of MB-RS4-Se (IV) was shown in Figure 5. The results indicated that the solubility and

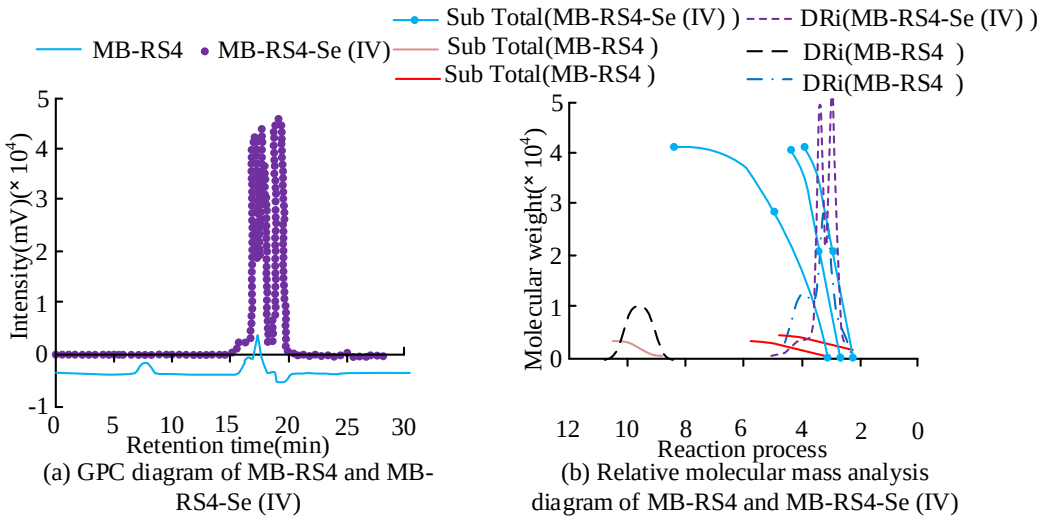

(a) GPC diagram of MB-RS4 and MB-RS4-Se (IV)

(b) Relative molecular mass analysis diagram of MB-RS4 and MB-RS4-Se (IV)

Figure 4. The results of gel permeation chromatography (GPC) and relative molecular mass analysis of MB-RS4 and MB-RS4·Se (IV).

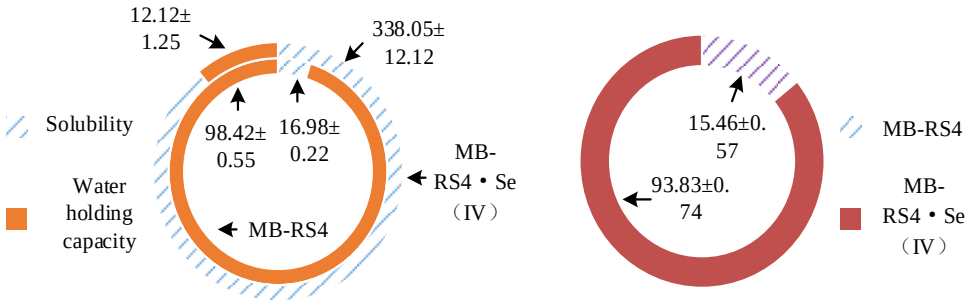

(a) Comparison of solubility and water holding capacity between MB-RS4 • Se (IV) and MB-RS4

(b) MB-RS4 • Se (IV) and MB-RS4 transparency results

Figure 5. Analysis of physical characteristics of MB-RS4-Se (IV).

Table 1. Relative molecular weight distribution before and after improvement.

			Mn (g/mol)	Mw (g/mol)	Mw_{10}	Mw_{90}	Mw/Mn
MB-RS4	Peaking	Peak 1 (×10^9)	5.95	8.16	14.59	3.30	1.37×10^{-9}
		Peak 2 (×10^3)	5.73	7.04	3.54	11.8	1.23×10^{-3}
	Non peaking	(×10^2)	22.6	1.85×10^7	9.91	7.74×10^7	8.3×10^3
MB-RS4·Se (IV)	Peaking	Peak 1 (×10^3)	10.9	14.4	6.61	25.8	1.31×10^{-3}
	Non peaking	(×10^2)	1.3	1.17	0.44	20.9	9.22×10^{-2}

transparency of MB-RS4·Se (IV) were significantly improved after selenization treatment, which might be due to the disruption of RS4 by nitric acid during the selenization process, resulting in the breakdown of the network structure within its particles. Therefore, the molecular weight was greatly reduced, resulting in an increase in solubility. while its binding effect on water molecules weakened and its ability to maintain water decreased.

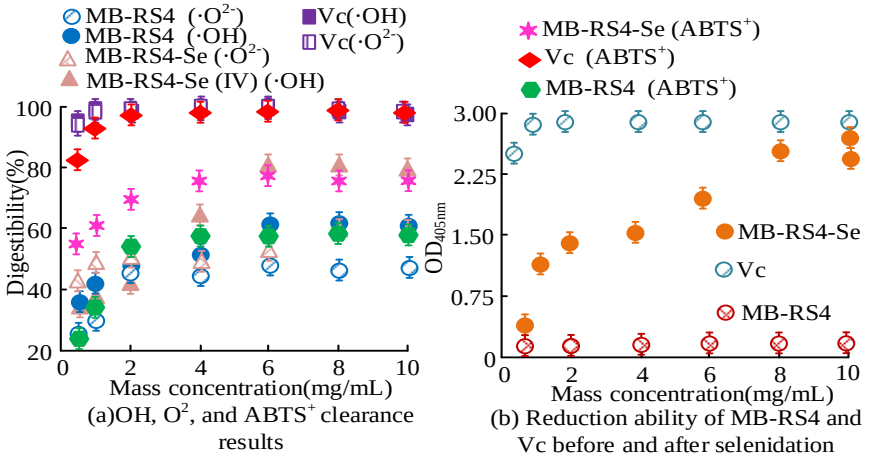

Figure 6. Analysis of antioxidant activity of MB-RS4 before and after selenization *in vitro*.

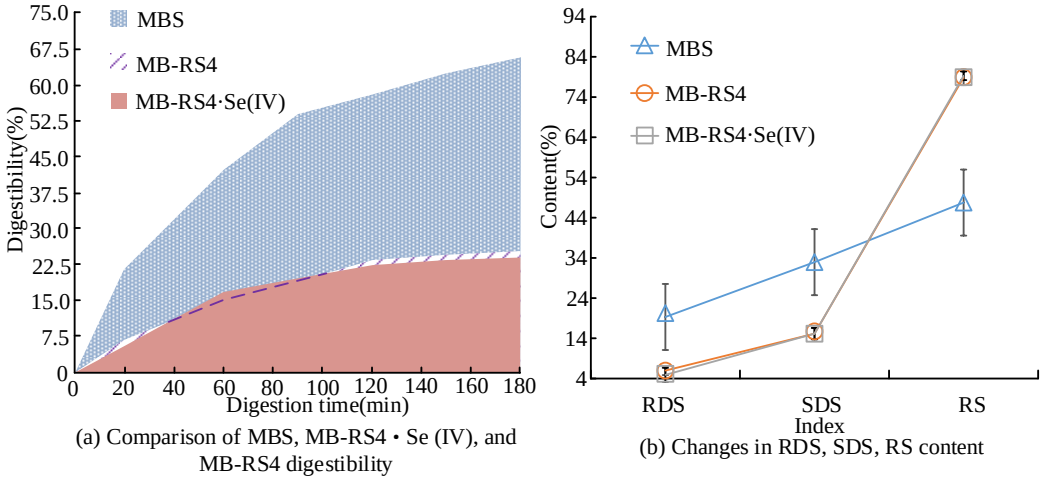

Figure 7. Digestibility comparison of the contents of rapid digestion of starch (RDS), slow digestion of starch (SDS), and resistant starch (RS).

Analysis of biological activity of selenized mung bean starch

The *in vitro* antioxidant activity of MB-RS4-Se (IV) was analyzed in Figure 6. The results demonstrated that there was a significant scavenging ability for ·OH, $\cdot O^{2-}$, and ABTS+ before and after modification, and the mass concentration was directly proportional to the scavenging ability. When the mass concentration was 2 mg/mL, the scavenging ability of MB-RS4·Se (IV) for $\cdot O^{2-}$ and ABTS+ reached its maximum, while, when the mass concentration was 6 mg/mL, the scavenging ability for ·OH reached its maximum. In addition, at a mass concentration of 16 mg/mL, the absorption rate after selenization was similar to Vc. Overall, the scavenging ability of MB-RS4·Se (IV) for ·OH, $\cdot O^{2-}$, and ABTS+ was significantly higher than that before selenization, while significantly enhancing its reducing ability. The half maximum inhibitory concentration (IC50) of MB-RS4 before and after selenization were shown in Table 2. There was a significant linear relationship between the scavenging ability of ·OH, $\cdot O^{2-}$, and ABTS+ before and after selenization. The modified reduction ability was significantly improved and showed a similar pattern to the other three antioxidant indicators, with an R^2 of 0.89. In addition, MBS

Table 2. IC50 value of MB-RS4 before and after selenization.

	-	·OH	$·O^{2-}$	$ABTS^{+}$	Restorability
Linear equation	MB-RS4·Se (IV)	m=36.14j+5.35	m=47.14j+1.30	m=-15.49j+6.92	m=0.84j+0.12
	Vc	m=97.98j+0.02	m=97.51j+0.27	m=-13.62j+6.72	m=2.66j+0.02
	MB-RS4	m=39.38j+2.68	m=32.01j+2.06	m=-16.66j+6.89	m=0.10j+0.01
R^2	MB-RS4·Se (IV)	0.93	0.91	0.88	0.89
	Vc	0.91	0.91	0.87	0.91
	MB-RS4	0.92	0.97	0.87	0.85
IC50	MB-RS4·Se (IV) (mg/mL)	1.62±0.45	1.43±0.19	0.23±0.26	
	Vc (mg/mL)	0.01±0.01	0.02±0.01	0.09±0.02	
	MB-RS4 (mg/mL)	2.44±0.76	8.39±1.29	4.05±1.04	

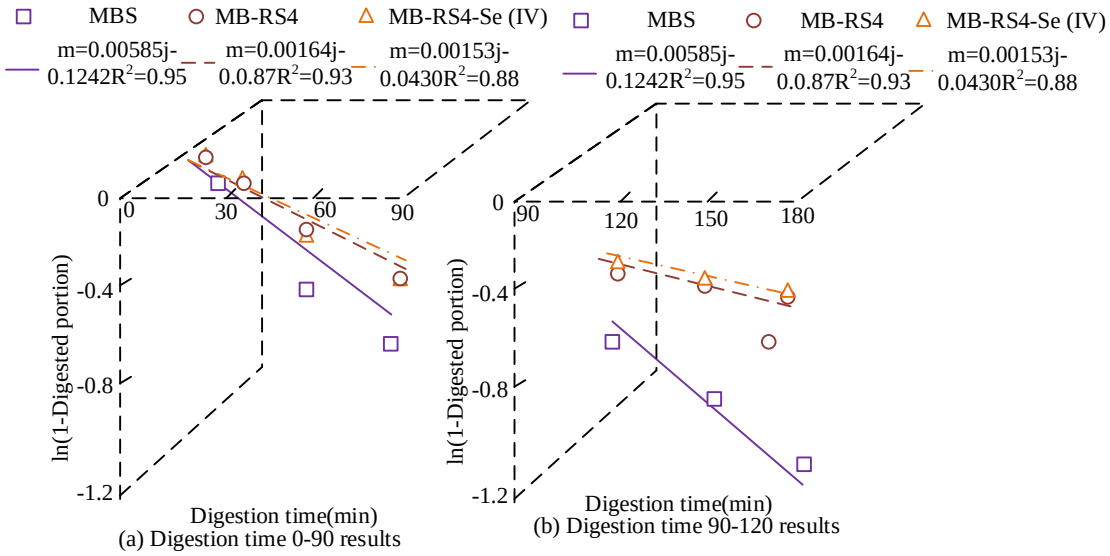

Figure 8. First order kinetic fitting results for MBS, MB-RS4, and MB-RS4 Se (IV).

was introduced as a control for the *in vitro* anti enzymatic hydrolysis characteristics in the analysis of the biological activity of MB-RS4·Se (IV). The digestibility and the changes in the content of rapid digestion of starch (RDS), slow digestion of starch (SDS), and resistant starch (RS) were shown in Figure 7. The results showed that digestion rate of MBS demonstrated an upward trend before 120 minutes, while the growth rate slowed down after 120 minutes. The digestibility of MB-RS4 and MB-RS4·Se (IV) remained low after 20 minutes with a small increase. In MBS, the contents of RDS and SDS were relatively high, while the proportion of RS was very low. However, the content of RS in MB-RS4 and MB-RS4 Se (IV) was significantly higher, resulting in a slower digestion rate for both. Overall, both MB-RS4 and MB-RS4·Se (IV) demonstrated strong anti-enzymatic degradation activities. The RS value of MB-RS4·Se (IV) was 79.29 ± 1.06, indicating higher anti-enzymatic degradation activity. A detailed analysis of the first-order dynamic fitting of the three was conducted. Figure 8 showed that the measurement coefficient R^2 values obtained by fitting the three were 0.95, 0.93, and 0.88, respectively. The degradation rate of MBS was much faster than that of MB-RS4 and MB-RS4·Se (IV). Overall, the degradation rates of MB-RS4 and MB-RS4·Se (IV) were basically consistent under different conditions, which indicated that particle size was not a key factor affecting enzymatic hydrolysis,

and the main reason limiting its degradation was the interaction between the enzyme and the substrate. In addition, the results of its inhibitory effects on α−glucosidase and α−amylase were illustrated in Figure 9. As the concentration increased, the inhibitory effect of MB-RS4 on α−glucosidase showed a negative change with no significant inhibitory effect. The IC50s of MB-RS4 and MB-RS4·Se (IV) were 4.99 mg/mL and 2.68 mg/mL, respectively. The inhibitory effect of MB-RS4·Se (IV) on α−glucosidase and α−amylase increased and stabilized in a concentration dependent manner. Overall, selenization modification transformed the non-inhibitory effect of MB-RS4 on α−glucose into an inhibitory effect, which might be due to the introduction of selenium that increased in molecular weight.

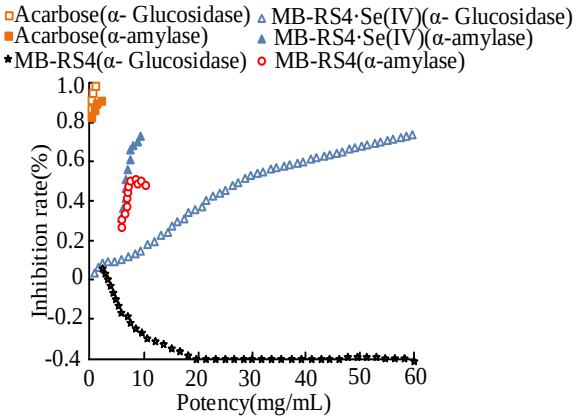

Figure 9. The inhibition of α-glucosidase and α-amylase by MB-RS4 and MB-RS4·Se (IV).

Further study was therefore needed to determine the types of inhibition of α−glucosidase and α−amylase. The results were shown in Figure 10. The results demonstrated that the increase in concentration of MB-RS4·Se (IV) led to an increase in K_m and a decrease in V_{max}, indicating that MB-RS4·Se (IV) was a competitive inhibitor of α−glucosidase. When the concentrations of MB-RS4 and MB-RS4·Se (IV) increased, both K_m and V_{maz} decreased. At each concentration, the fitting curve of enzyme catalysis rate of MB-Rs4 and MB-RS4·Se (IV) would coincide in the third quadrant, which indicated that MB-RS4 and MB-RS4·Se (IV) belonged to a mixed type of anticompetitive inhibition on α−amylase.

Conclusion

To effectively reduce the damage caused by traditional starch intake to the human body, this study used mung bean starch (MBS) as the research object and citric acid to esterification MBS to prepare MB-RS4. The preparation conditions of MB-RS4·Se (IV) using nitric acid sodium selenite were studied, and the structural characterization and biological activity of MB-RS4·Se (IV) were analyzed. The results showed that the optimized material ratio, optimal esterification temperature, and optimal esterification time for MB-RS4·Se (IV) preparation process were 1:1, 66°C, and 3.5 h, respectively, with a success rate of 26.451%. In the structural investigation, the results showed that the crystal structure of modified MB-RS4·Se (IV) was destroyed, and its molecular weight decreased. In the biological activity analysis, the scavenging ability of MB-RS4·Se (IV) for $\cdot O^{2-}$ and ABTS+ reached its highest level at a mass concentration of 2 mg/mL after selenization, and the scavenging ability for ·OH reached its highest at a mass concentration of 6 mg/mL, while the absorbance value was close to the positive control Vc at a mass concentration of 10 mg/mL. The RS value of MB-RS4·Se (IV) was 79.29 ± 1.06, which was higher than that of MBS and MB-RS4, and it has high anti-enzymatic degradation activity. Meanwhile, the inhibitory effect of MB-RS4·Se (IV) on α−glucosidase and α−amylase increased and stabilized after selenization. The types of repression were competitive repression and mixed anti-competitive repression. Overall, the experimental modified MB-RS4·Se (IV) had a smaller molecular weight and antioxidant and anti-enzymatic capabilities, which was effective in clearing harmful free radicals from the human body. However, the study did not explore the mechanisms of the inhibitory effect of enzymes, and further analysis is needed.

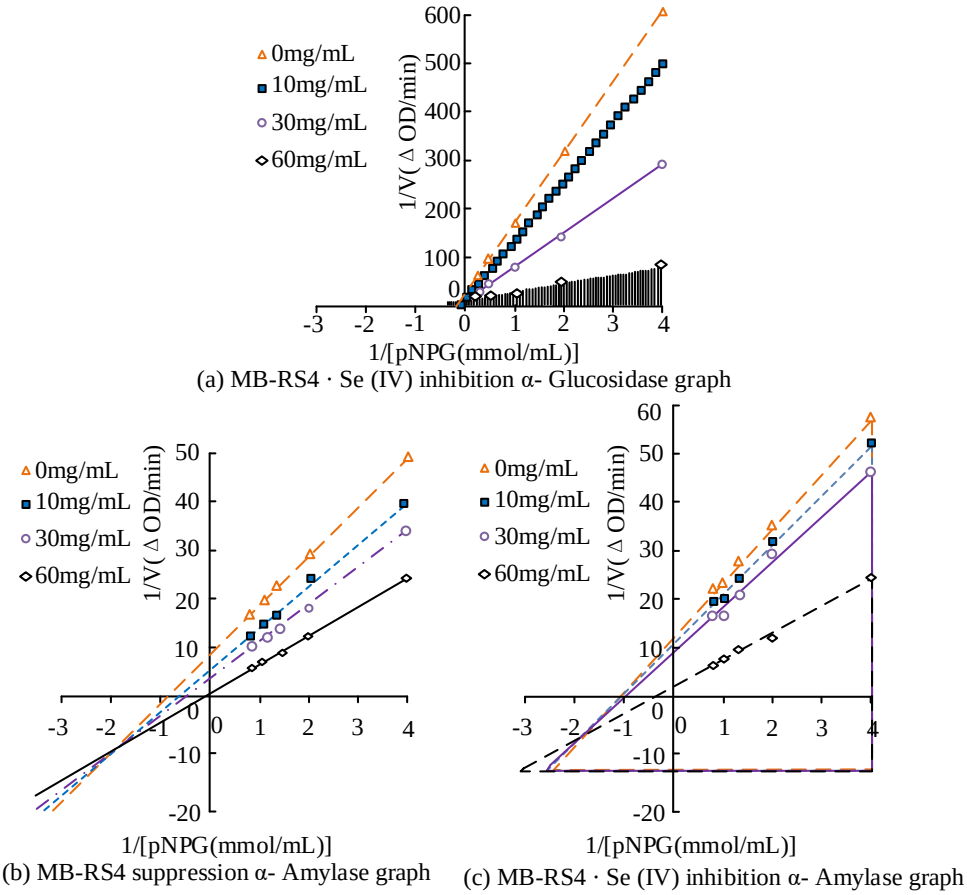

Figure 10. Analysis of MB-RS4 and MB-RS4·Se (IV) inhibition type on α-glucosidase and α-amylase inhibition.

References

1. Zhang K, Dai Y, Hou H, Li X, Zhang H. 2019. Influences of grinding on structures and properties of mung bean starch and quality of acetylated starch. Food Chem. 294(1):285-292.
2. Moran Jr ET. 2019. Starch: Granule, amylose-amylopectin, feed preparation, and recovery by the fowl's gastrointestinal tract. J Appl Poultry Res. 28(3):566-586.
3. Song YX, Min YT, Ma QY. 2019. Preparation and study on *in vitro* hypoglycemic activity of a new resistant starch with α-amylase inhibitory groups. Food Res Int. 45(9):103-107.
4. Wang L, Chen J, Lu S, Xiao P, Li C, Yi C. 2022. Structural characterization, physicochemical properties and *in vitro* digestion of finger millet–resistant starch prepared by different methods. Int J Food Sci Tech. 57(1):416-425.
5. Arp CG, Correa MJ, Ferrero C. 2020. Production and characterization of type III resistant starch from native wheat starch using thermal and enzymatic modifications. Food Bioprocess Tech. 13(7):1181-1192.
6. Patterson MA, Maiya M, Stewart ML. 2020. Resistant starch content in foods commonly consumed in the United States: A narrative review. J Acad Nutr Diet. 120(2):230-244.
7. Xu J, Ma Z, Li X, Liu L, Hu X. 2020. A more pronounced effect of type III resistant starch *vs*. type II resistant starch on ameliorating hyperlipidemia in high fat diet-fed mice is associated with its supramolecular structural characteristics. Food Funct. 11(3):1982-1995.
8. Denchai N, Suwannaporn P, Lin J, Soontaranon S, Kiatponglarp W, Huang TC. 2019. Retrogradation and digestibility of rice starch gels: the joint effect of degree of gelatinization and storage. J Food Sci. 84(6):1400-1410.
9. Ye J, Luo S, Huang A, Chen J, Liu C, McClements DJ. 2019. Synthesis and characterization of citric acid esterified rice starch by reactive extrusion: A new method of producing resistant starch. Food Hydrocolloid. 92(6):135-142.
10. de Azevedo LC, Rovani S, Santos JJ, Dias DB, Nascimento SS, Oliveira FF, *et al*. 2020. Biodegradable films derived from corn and potato starch and study of the effect of silicate extracted from sugarcane waste ash. ACS Appl Polym Mater. 2(6):2160-2169.
11. Li T, Teng H, An F, Huang Q. Chen L, Song H. 2019. The beneficial effects of purple yam (*Dioscorea alata L*.) resistant starch on hyperlipidemia in high-fat-fed hamsters. Food Funct. 10(5):2642-2650.

12. Sharma S, Sharma S, Bharti AS, Tiwari MK, Uttam KN. 2023. Non-destructive assessment of the nutrient profile of underutilized seeds using spectroscopic probes. Anal Lett. 56(5):703-719.
13. Yang W, Huang G, Chen F, Huang H. 2021. Extraction/synthesis and biological activities of selenopolysaccharide. Trends Food Sci Tech. 109(1):211-218.
14. Li Q, Yang S, Chen F, Guan W, Zhang S. 2022. Nutritional strategies to alleviate oxidative stress in sows. Anim Nutr. 9(2):60-73.
15. Zhang RR, Jiao SF, Liu ZJ, Zheng YY, Yin YZ, Liang XT, *et al*. 2022. Construction of starch-based bionic glutathione peroxidase and its catalytic mechanism. Chem Pap. 76(6):3499-3506.
16. Passaretti MG, Ninago MD, Villar MA, López O. 2022. Thermoplastic starch and mica clay composites as biodegradable mulching films. J Polym Environ. 30(10):4394-4405.
17. Hu Y, Zhang Q, Garcia-Rojas D, Ling V, Masterson CM, Bi Y, *et al*. 2022. Increasing the antioxidant capacity of ceria nanoparticles with catechol-grafted poly (ethylene glycol). J Mater Chem B. 10(48):10042-10053.
18. Abuelizz HA, Anouar EH, Marzouk M, Taie HA, Ahudhaif A, Al-Salahi R. 2020. DFT study and radical scavenging activity of 2-phenoxypyridotriazolo pyrimidines by DPPH, ABTS, FRAP and reducing power capacity. Chem Pap. 74(9):2893-2899.